Production of $N_2(B^3\Pi_g, v'=1-12)$ in the Reaction between $NF(a^1\Delta)$ and $N(^2D)$

Steven J. Davis and Lawrence G. Piper*

Physical Sciences Inc., 20 New England Business Center, Andover, Massachusetts 01810
(Received: August 9, 1989; In Final Form: January 4, 1990)

Simultaneous determination of the absolute number densities of $N(^2D)$, NF(a), and $N_2(B^3\Pi_g, v'=1-12)$ in a discharge flow reactor yielded rate coefficients for the reaction $N(^2D) + NF(a) \rightarrow N_2(B, v'=1-12) + F$ of $(2.5 \pm 1.1) \times 10^{-10}$ cm^3 molecule^{-1} s^{-1}. We also observed Vegard–Kaplan emission from the reaction of $N(^2D)$ with NF(a). Most of the $N_2(A)$ formation, however, appears to result from radiative cascade from the $N_2(B)$ rather than as the result of a direct channel.

I. Introduction

In 1970, Clyne and White observed excited molecular nitrogen production from a sequence of reactions beginning with the reaction of H with NF_2.[1] This reaction sequence also produced $NF(a^1\Delta)$ and $NF(b^1\Sigma)$. They suggested that $N(^4S)$ atom recombination was the source of $N_2(B)$.

In 1973 Herbelin and Cohen[2] performed a similar chemiluminescence study and suggested the following mechanism:

$$H + NF_2 \rightarrow NF(a) + HF \quad (1)$$

$$H + NF(a) \rightarrow N(^2D) + HF \quad (2)$$

$$N(^2D) + NF(a) \rightarrow N_2(B) + F \quad (3)$$

Although they could not prove this model, they presented indirect evidence for its validity and argued that spin and angular momentum conservation would be major constraints in reaction product channel availability. In particular, they emphasized that the reaction of H + NF(a) would produce $N(^2D)$ exclusively if these correlation rules held rigorously. In spite of these early observations, the reaction mechanism for this potentially important source of N_2^* has remained unclear.

In the early 1980s Clyne and co-workers embarked on a series of detailed experiments designed to clarify this interesting reaction sequence.[3–5] Using sensitive diagnostic techniques, they observed that $N(^2D)$ was indeed the primary product of reaction 2 and showed that $N_2(B)$ fluorescence rates varied linearly with the product of the number densities of $N(^2D)$ and $NF(a^1\Delta)$. They concluded, therefore, that Herbelin and Cohen's proposed mechanism was probably correct. In addition, they estimated a rate coefficient for reaction 2 of 2.5×10^{-13} cm^3 molecule^{-1} s^{-1} and suggested that $N_2(B)$ photon emission rates were consistent with a one-tenth gas kinetic rate for reaction 3, i.e., $k_3 \sim 3 \times 10^{-11}$ cm^3 molecule^{-1} s^{-1}.

In a recent study,[6] where we monitored directly the decay of NF(a) in the presence of H, we found $k_2 = (3.1 \pm 0.6) \times 10^{-13}$ cm^3 molecule^{-1} s^{-1}. This report details simultaneous quantitative measurements of absolute number densities of $N(^2D)$, NF(a), and $N_2(B^3\Pi_g, v'=1-12)$. From these data we determine the rate coefficient for reaction 3.

II. Experimental Section

The 5-cm-i.d. flow reactor used in these studies has been described previously.[6] NF(a) and $N(^2D)$ both were produced chemically. NF_2, produced in a weak microwave discharge through NF_3 dilute in Ar or He, mixed downstream with a flow of H_2. Fluorine atoms from the NF_3 discharge reacted with the H_2 to generate H atoms and HF. The H atoms then reacted with the NF_2 to make NF(a) via reaction 1 and subsequently with the NF(a) to make $N(^2D)$ via reaction 2. The $N(^2D)$ then reacted with residual NF(a) to make $N_2(B^3\Pi_g)$. Simultaneous determination of [NF(a)], $[N(^2D)]$, and $[N_2(B)]$ sufficed to determine k_3 (vide infra).

NF(a) and $N_2(B)$ were monitored spectroscopically with a 0.3-m monochromator coupled to a thermoelectrically cooled, GaAs photomultiplier. The system was calibrated to make absolute, photon emission rate measurements by observing the O/NO air afterglow under carefully controlled conditions. We have detailed our calibration procedures previously.[7,8]

$N(^2D)$ was detected by resonance fluorescence using a microwave discharge resonance lamp and a 0.2-m vacuum-UV monochromator coupled to a solar blind photomultiplier tube.[9] The resonance fluorescence detection system was calibrated to give absolute $N(^2D)$ number densities by correlating fluorescence intensities with $N(^2D)$ number densities that were determined by resonance absorption measurements (vide infra). The absorption measurements used a second discharge lamp that was attached to the flow tube opposite the vacuum-UV monochromator. The fluorescence lamp was normal to both the monochromator and the absorption lamp. The absorption lamp was run at a microwave power of 20 W in 1.5 Torr of He with a trace of N_2 (introduced through a Granville Phillips calibrated leak valve). Previous studies[10] showed that these conditions produced gas temperatures in the lamp of ~600 K.

A dielectric-coated filter (MgF_2 substrate) in front of the resonance fluorescence lamp rejected the 174.3-nm line while passing the line at 149.3 nm. This procedure discriminates against detection of $N(^2P)$ metastables which absorb 174.3-nm radiation. By placing the filter on the absorption lamp, we determined that the ratio of the intensity at 174.3 nm to that at 149.3 nm was approximately 0.01. This level of discrimination was adequate for the present studies.

The resonance fluorescence lamp calibration involved constructing a curve of growth for $N(^2D)$. A microwave discharge through a flow of N_2 dilute in Ar produced $N(^2D)$ in the flow tube for the calibration experiments. Resonance absorption on the 149.3-nm line determined the number density of $N(^2D)$, and these number densities were correlated with simultaneous measurements of $N(^2D)$ resonance fluorescence. Adding varying flows of CO_2 to the reactor quenched some of the $N(^2D)$ and thereby served to vary its number density. Figure 1 shows a typical calibration plot.

Experimental runs consisted of scans of the chemiluminescence due to $N_2(B \rightarrow A)$ and $NF(a \rightarrow X)$ along with a determination of $[N(^2D)]$ at the same spatial position. Several such measurements were repeated for different H_2 flows with all other conditions held constant. Most experiments use a fixed H_2 injector, but one set

* Author to whom correspondence should be addressed.

(1) Clyne, M. A. A.; White, I. F. *Chem. Phys. Lett.* **1970**, *6*, 465.
(2) Herbelin, J. M.; Cohen, N. *Chem. Phys. Lett.* **1973**, *20*, 605.
(3) Cheah, C. T.; Clyne, M. A. A.; Whitefield, P. D. *J. Chem. Soc., Faraday Trans. 2* **1980**, *76*, 711.
(4) Cheah, C. T.; Clyne, M. A. A. *J. Chem. Soc., Faraday Trans. 2* **1980**, *76*, 1543.
(5) Cheah, C. T.; Clyne, M. A. A. *J. Photochem.* **1981**, *15*, 21.
(6) Davis, S. J.; Rawlins, W. T.; Piper, L. G. *J. Phys. Chem.* **1989**, *93*, 1078.
(7) Piper, L. G.; Caledonia, G. E.; Kennealy, J. P. *J. Chem. Phys.* **1981**, *75*, 2847.
(8) Piper, L. G. *J. Chem. Phys.* **1988**, *88*, 231.
(9) Piper, L. G.; Donahue, M. E.; Rawlins, W. T. *J. Phys. Chem.* **1987**, *91*, 3883.
(10) Rawlins, W. T.; Piper, L. G. *Proc. Soc. Photo.-Opt. Instrum. Eng.* **1981**, *279*, 58.

0022-3654/90/2094-4515$02.50/0

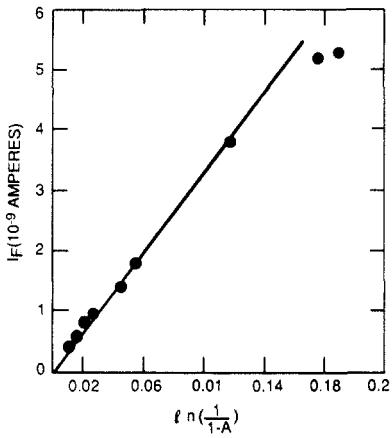

Figure 1. Plot of $N(^2D)$ resonance fluorescence signal, I_F, versus ln $(1/1 - A)$. A is the fractional absorption. The abscissa is directly proportional to $N(^2D)$ number density.

used a sliding H_2 injector. The bath gas pressure (0.7–3.2 Torr), bath gas species (Ar and He), and flow velocity (1.1×10^3 to 5.5×10^3 cm s^{-1}) were varied from one series of runs to another. The chemiluminescence spectra were recorded on a COMPAQ microcomputer and stored for later analysis using a spectral-fitting code. The spectral-fitting routine incorporated the absolute spectral response calibration data; consequently, it calculated absolute number densities for the species $N_2(B)$, NF(a), and NF(b). The Einstein coefficients used to convert observed photon emission rates to number densities came from Lofthus and Krupenie[11] for $N_2(B)$, Tennyson et al.[12] for NF(b), and Malins and Setser[13] for NF(a). Since $v' = 0$ in $N_2(B)$ could not be detected, the results are for $N_2(B;v=1-12)$.

When reaction 1 is run in excess hydrogen, copious amounts of HF overtone ($HF^\dagger$) emission are produced via reaction 2. In our experiments, we formed NF_2 by subjecting NF_3 to a weak discharge as described above. The discharge also produced atomic fluorine to which we added H_2. The H_2 + F reaction not only served as a convenient source of H but also acted as an additional source of vibrationally excited HF. The (3,0) HF overtone band is contained within the same wavelength region as the NF(a–X) chemiluminescence near 874 nm. This spectral contamination can result in errors in the extraction of NF(a) number densities from the chemiluminescence data. The HF overtone emission, however, could be quenched to undetectable levels by adding sufficient H_2, molecular hydrogen being an efficient quencher of $HF^\dagger$, but with no diminution in the NF(a) concentration. This procedure gave NF(a–X) spectra that were free from any detectable HF overtone emission.

The $HF^\dagger$ spectral overlap with NF(a–X) emission became a problem at short reaction times using the sliding injector. Data recorded from 0 to 2.5 ms downstream from the H_2 injector were heavily contaminated with HF(3,0) emission. Consequently, only those NF(a) data for $t > 2.5$ ms were used. The relatively clean NF(a→X) spectra taken between 2.5 and 10 ms gave an excitation rate for $N_2(B)$ in good agreement with all fixed H_2 injector data.

The $N_2(B\rightarrow A)$ (2,1) and NF(a→X) (0,0) band chemiluminescence emissions also occur in the same spectral region. This overlap is a relatively minor problem, however, since the population of $N_2(B,v'=2)$ is determined redundantly by observing the (2,0) band near 770 nm.

III. Results

Figure 2 shows a typical chemiluminescence spectrum and corresponding synthetic fit. Prominent emission features originate from NF(a), NF(b), $N_2(B)$, and HF. Because the NF(b→X) (0,0) band at 528 nm was several times more intense than all other

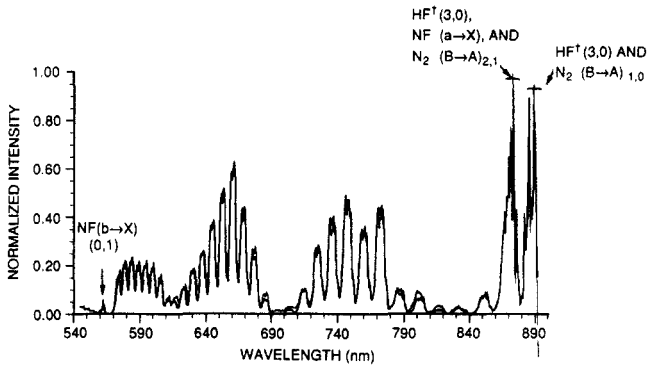

Figure 2. Chemiluminescence spectrum (thin line) showing NF(b→X), $N_2(B\rightarrow A)$, NF(a→X), and HF(3→0) systems. The thick line trace is a computer fit to the data derived from the spectral-fitting code.

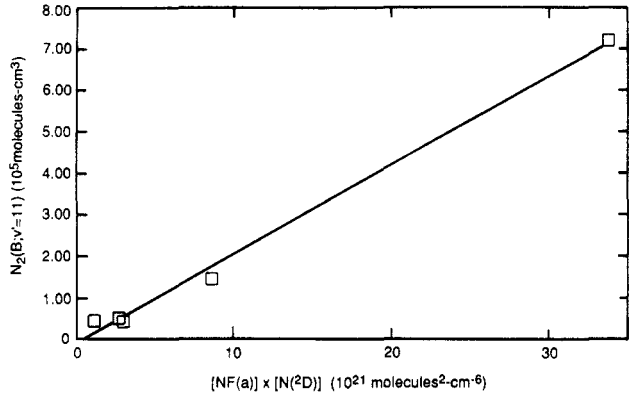

Figure 3. Plot showing linear dependence of $[N_2(B)]$ with respect to the product $[NF(a)][N(^2D)]$. Run conditions: pressure = 3.06 Torr of Ar bath gas.

features between 500 and 900 nm, the (0,1) band at 560 nm was used to monitor [NF(b)]. This approach allowed using a single sensitivity setting for an entire spectrum. In separate measurements we found that the NF(b–X) (0,1) band was 33 ± 2 times weaker than the (0,0) band.

The rate of change of $[N_2(B)]$ with the time is given by

$$d[N_2(B)]/dt = k_3[NF(a)][N(^2D)] - [N_2(B)](A_{B\rightarrow A} + K_Q) \quad (4)$$

where $A_{B\rightarrow A}$ is the radiative rate for N_2 first-positive emission and K_Q is the effective first-order quenching rate of $N_2(B)$ by species in the flow. Because $N_2(B)$'s radiative decay rate is rapid compared to its residence time in the observation region, it is in steady state. The term $d[N_2(B)]/dt$ in eq 4, therefore, vanishes, and we find

$$[N_2(B)] = \frac{k_3[NF(a)][N(^2D)]}{A_{B\rightarrow A} + K_Q} \quad (5)$$

A plot of $[N_2(B)]$ versus the product of $[NF(a)][N(^2D)]$ should be linear with a slope of $k_3/(A_{B\rightarrow A} + K_Q)$.

Figure 3 shows a typical plot of $[N_2(B,v'=11)]$ versus $[NF(a)][N(^2D)]$. Note that the $[NF(a)][N(^2D)]$ product varies by nearly 2 orders of magnitude. The slope of this plot should equal $k_3^{v=11}/(A_{B\rightarrow A} + K_Q)$. The total excitation rate coefficient, k_3, will be the sum of the production rates into the individual vibrational levels of $N_2(B)$:

$$k_3 = \sum_{i=0}^{12} k_3^{v_i} \quad (6)$$

Plots similar to Figure 3 gave the excitation rate coefficients for each vibrational level. Since we could not monitor $v' = 0$, the k_3 we present is only for levels $v' = 1-12$. This results in an underestimate of the total k_3 of about 16% (vide infra).

Figures 4 and 5 summarize the state-specific rate coefficients in He and Ar bath gases, respectively, and show how they vary

(11) Lofthus, A.; Krupenie, P. H. *J. Phys. Chem. Ref. Data* **1977**, *6*, 287.
(12) Tennyson, P. H.; Fontijn, A.; Clyne, M. A. A. *Chem. Phys.* **1981**, *62*, 171.
(13) Malins, R. J.; Setser, D. W. *J. Phys. Chem.* **1981**, *85*, 1342.

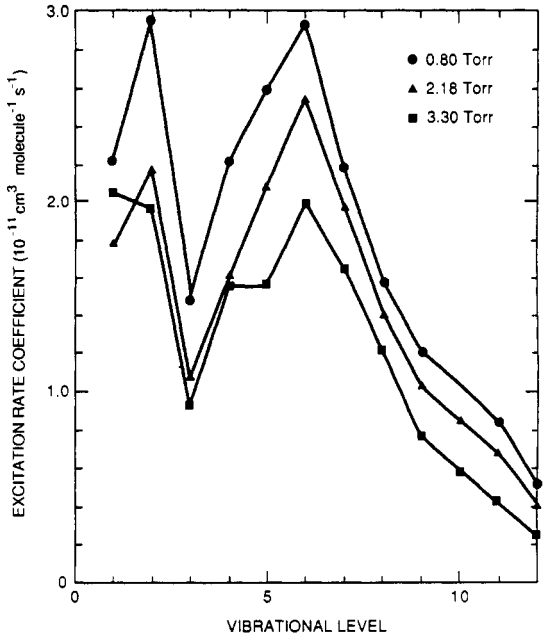

Figure 4. Dependence of excitation rate coefficient, k_3^v, as a function of v' for three different helium pressures.

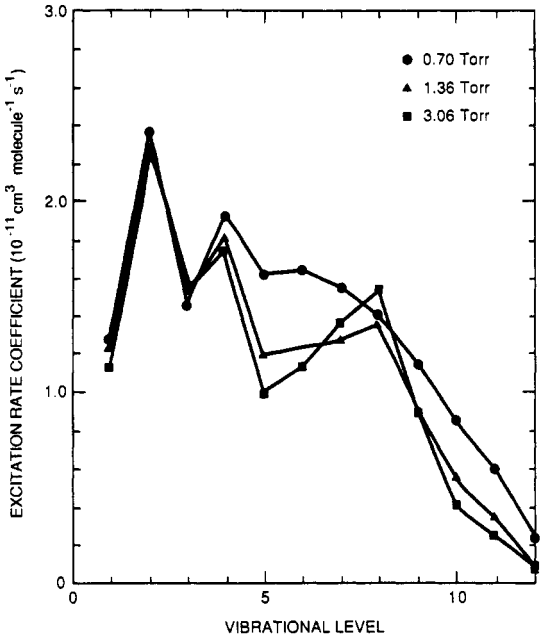

Figure 5. Dependence of k_3^v as a function of v' for three different argon pressures.

with bath gas pressure. The data show signs of bath gas electronic quenching. Furthermore, the relative vibrational distributions change markedly with pressure in argon, whereas they show little variation with pressure in helium. We have observed previously in $N_2(A)$ energy-pooling studies that collisions with Ar will redistribute $N_2(B)$ vibrational distributions, leading to enhanced populations in $v' = 8$ at higher pressures.[14] Similar redistributions in $N_2(B,v)$ populations have also been observed by several groups studying N atom recombination in Ar.[15-17] In our own N atom recombination studies,[18] we have not observed similar strong changes in $N_2(B,v)$ with pressure when He was the buffer gas. We think, therefore, that the vibrational distributions measured

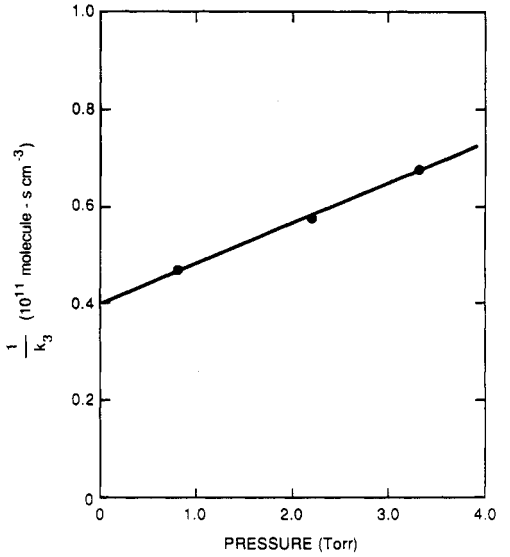

Figure 6. Variation in the reciprocal of the total $N_2(B)$ excitation rate coefficient with pressure of helium bath gas.

TABLE I: Relative Rate Coefficients for Excitation of $N_2(B,v)$ in the Reaction between $N(^2D)$ and $NF(a^1\Delta)$

v'	$k_3^v/\sum_{v=1}^{12} k_3^v$	v'	$k_3^v/\sum_{v=1}^{12} k_3^v$	v'	$k_3^v/\sum_{v=1}^{12} k_3^v$
1	0.113 ± 0.021	5	0.114 ± 0.008	9	0.055 ± 0.004
2	0.131 ± 0.007	6	0.138 ± 0.006	10	0.045 ± 0.006
3	0.064 ± 0.004	7	0.107 ± 0.006	11	0.035 ± 0.006
4	0.100 ± 0.007	8	0.078 ± 0.005	12	0.021 ± 0.004

in He may be close to nascent. They clearly are not in the Ar bath gas studies. We do not feel that reliable results on $N_2(B)$ formation in chemiluminescent systems can be obtained in experiments employing an argon buffer.

We focused, therefore, on the results obtained in helium. Figure 6 shows the reciprocal of the total $N_2(B)$ excitation rate coefficient plotted as a function of helium pressure. The intercept of the plot gives the excitation rate coefficient in the absence of quenching, while the slope gives the ratio of the helium quenching rate coefficient to the radiative decay rate. The extrapolated rate coefficient for reaction 3 is 2.5×10^{-10} cm^3 molecule^{-1} s^{-1}. The slope indicates a half-quenching pressure of $N_2(B)$ by helium of 5 Torr. The relative rate coefficients for the individual vibrational levels measured in the helium runs were averaged. Table I summarizes the results.

The major sources of error reside in the calibrations for the $[N(^2D)]$, $[NF(a)]$, and $[N_2(B)]$ diagnostics. The NO/O calibration procedure introduces a 29% root-mean-square error: 25% for the O + NO rate coefficient[19-25] and 15% reproducibility in the measurements of the NO/O titration. The estimated error in the $N(^2D)$ calibration is ~15%. The reported value of the NF(a) lifetime probably carries an additional 25% error.[13] Combining these in quadrature with statistical uncertainties results in an overall uncertainty of ~42%. This apparently large uncertainty primarily results from the errors quoted in the literature for results necessary to reduce the data.

IV. Discussion

A. Identification of Reaction Sequence. While our reaction mixture contains a number of reactive species, only five possible

(14) Piper, L. G. *J. Chem. Phys.* **1988**, *88*, 6911.
(15) Bayes, K. D.; Kistiakowski, G. D. *J. Chem. Phys.* **1960**, *32*, 992.
(16) Brown, R. L. *J. Chem. Phys.* **1970**, *52*, 4604.
(17) Becker, K. H.; Fink, E. H.; Groth, W.; Jud, W.; Kley, D. *Discuss. Faraday Soc.* **1972**, *53*, 35.
(18) Piper, L. G. Unpublished results, 1987.
(19) Fontijn, A.; Meyer, C. B.; Schiff, H. I. *J. Chem. Phys.* **1964**, *40*, 64.
(20) Vanpee, M.; Hill, K. D.; Kineyko, W. R. *AIAA J.* **1971**, *9*, 135.
(21) Golomb, D.; Brown, J. H. *J. Chem. Phys.* **1975**, *63*, 5246.
(22) Woolsey, G. A.; Lee, P. H.; Slafer, W. D. *J. Chem. Phys.* **1977**, *67*, 1220.
(23) Sutoh, M.; Morioka, Y.; Nakamura, M. *J. Chem. Phys.* **1980**, *72*, 20.
(24) Pravilov, A. M.; Smirnova, L. G. *Kinet. Catal.* (*Engl. Transl.*) **1978**, *19*, 202.
(25) Bradburn, G.; Lilenfeld, H. *J. Phys. Chem.* **1988**, *92*, 5266.

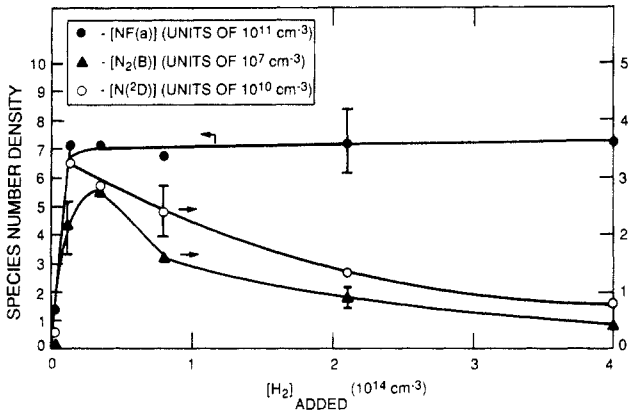

Figure 7. Plot of [NF(a)], [N_2(B)], and [N(^{2}D)] as functions of [H_2] added. Total pressure = 3.06 Torr (Ar); effective reaction time = 17.3 ms.

reactions can lead to N_2(B) formation, and three of those lack sufficient exoergicity to excite more than a few of the lowest vibrational levels of N_2(B). These reactions are

$$N(^4S) + NF(a^1\Delta) \rightarrow N_2(B^3\Pi_g, v' \leq 1) + F(^2P) \quad (7)$$

$$N(^4S) + NF(b^1\Sigma^+) \rightarrow N_2(B^3\Pi_g, v' \leq 6) + F(^2P) \quad (8)$$

$$N(^2D) + NF(X^3\Sigma^-) \rightarrow N_2(B^3\Pi_g, v' \leq 6) + F(^2P) \quad (9)$$

$$N(^2D) + NF(a^1\Delta) \rightarrow N_2(B^3\Pi_g, v') + F(^2P) \quad (3)$$

$$N(^2D) + NF(b^1\Sigma^+) \rightarrow N_2(B^3\Pi_g, v') + F(^2P) \quad (10)$$

The first three of these reactions lack sufficient exoergicity to account for the excitation we see of N_2(B) and $N_2(a^1\Pi_g)$ up to the dissociation limit. Furthermore, observations of N(^{4}S) temporal profiles (vide infra) show that this species cannot be linked kinetically to the formation of N_2(B).

The number densities of NF($b^1\Sigma^+$) generally are 2 orders of magnitude smaller than those of NF(a). Since k_3 already is gas kinetic, the rate coefficient for reaction 10 would have to be 100 times gas kinetic to be able to compete with reaction 3. The following paragraphs establish the kinetic linkage between N(^{2}D), NF($a^1\Delta$), and $N_2(B^3\Pi_g)$.

Figure 7 shows the variation of number densities of various excited species with the amount of H_2 added. The [NF(a)] seems to reach a steady value, independent of [H_2], as observed previously.[6] In contrast, [N(^{2}D)] and [N_2(B)] first increase and then decay in a manner consistent with the measured quenching of N(^{2}D) by H_2.[9,26] If H_2 were quenching N_2(B) directly, a quenching rate coefficient of $\sim 10^{-9}$ cm^3 molecule^{-1} s^{-1} would be required to explain its observed decay. Thus, the H_2 must be quenching N(^{2}D), the precursor of N_2(B).

Since N_2(B) is in steady state with N(^{2}D), the ratio of [N_2(B)]/[N(^{2}D)] should be constant at constant [NF(a)]. In the plateau region of Figure 7 $\langle$[NF(a)]$\rangle$ = (7.1 ± 0.2) × 10^{11} molecules cm^{-3} and $\langle$[N_2(B)]/[N(^{2}D)]$\rangle$ = (7.2 ± 1.4) × 10^{-4}. All runs showed similar behavior. The value of [N_2(B)]/[N(^{2}D)] varied with [NF(a)], being larger for larger values of [NF(a)]. For any set of runs with constant [NF(a)], however, [N_2(B)]/[N(^{2}D)] was constant to within ±20%.

We also looked briefly for chemiluminescence in the ultraviolet and vacuum ultraviolet. We observed both Vegard–Kaplan, $N_2(A^3\Sigma_u^+-X^1\Sigma_g^+)$, and Lyman–Birge–Hopfield, $N_2(a^1\Pi_g-X^1\Sigma_g^+)$, emission, showing the presence of both N_2(A) and N_2(a) in the reaction mixture. The number densities of N_2(A) and N_2(a) varied with changes in the amount of H_2 added to a discharged NF_3 mixture in a manner similar to that observed for N(^{2}D) and N_2(B). It appears, therefore, that not only N_2(B) but also N_2(A) and

(26) Whitefield, P. D.; Hovis, F. E. *Chem. Phys. Lett.* **1987**, *135*, 454.

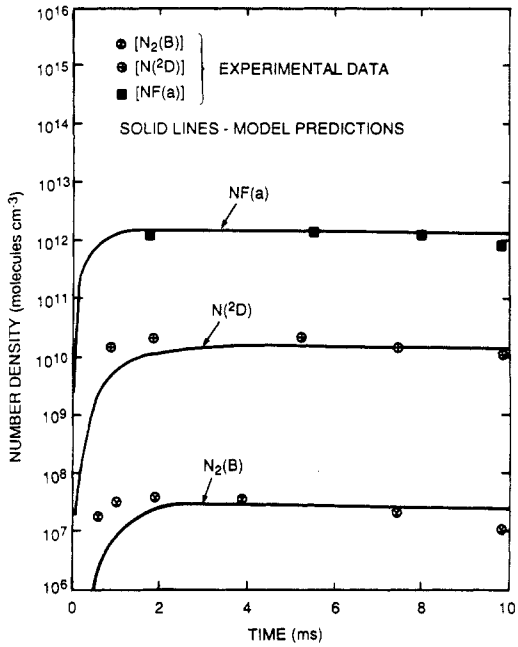

Figure 8. Comparison of predicted and measured population profiles for NF(a), N(^{2}D), and N_2(B). Total bath gas pressure was 2.2 Torr (He).

N_2(a) are formed either directly in reaction 3 or indirectly as a result of radiative cascade or quenching one of the principal products of reaction 3.

For completeness we also monitored, by resonance fluorescence at 120 nm, the temporal variation of relative N(^{4}S) number densities in our system. Figure 8 shows relative number density profiles for N(^{4}S) and N_2(B) (which as shown previously closely follows [N^2(D)]). It is clear that N(^{4}S) is not a primary reaction product and is only formed at relatively late reaction times. Its role in N_2* production can therefore be only minimal.

B. Computer Modeling. We modeled the H + NF_2 system to check the consistency of our observations and to provide insight into some experimental details. The modeling was completed using the code CHEMKIN. This code, developed by Lee et al.,[27] contains a differential equation solver and also allows sensitivity analyses to be performed, although we did not undertake such a study in this work. Typically, a sensitivity analysis is performed to identify the kinetic mechanisms that dominate a multistep process. Our study was concerned with measuring only a few kinetic rate coefficients, and we incorporated our values into a rate package described in ref 28. The purpose of this exercise was to compare the temporal profiles that we observed to those predicted by the model. We find temporal profiles from model predictions of the number densities of N_2(B), N(^{2}D), and NF(a) compare well with experimental data.

The model was run by specifying an initial set of conditions for all species concentrations. The rate equations were then integrated, and the species concentrations were predicted from 0 to 10 ms at 1-ms intervals. This range was identical with that of the experimental runs when the sliding injector was used. The model assumed that all species were premixed. The reactions considered and the corresponding rate package, that of Koffend et al.,[28] are presented in Table II.

Initial conditions in the model were chosen to be identical with those of the actual experiments. The $[Ar]_0$ and $[H_2]_0$ were measured directly from the mass flowmeter readings. The largest uncertainty in initial condition determination occurred for $[NF_2]_0$ and $[F]_0$. The concentrations of these were estimated since they could not be measured directly. The upper limit of the $[NF_2]_0$ was $[NF_3]_0$ while $[F]_0$ is required to be less than 3[NF_3]. Because

(27) Lee, R. J.; Miller, J. A.; Jefferson, T. H. Report SAND 80-8003; Sandia Laboratories: Albuquerque, NM, 1980.

(28) Koffend, J. B.; Gardner, C. E.; Heidner, R. F. Aerospace Report SD-TR-85-55, 1985.

TABLE II: Rate Package Used in Modeling Study

	reaction	rate coefficient[a]	this work[b]
(1)	$F + H_2 \rightarrow HF(1) + H$	7.30×10^{-11}	28
(2)	$F + H_2 \rightarrow HF(2) + H$	2.40×10^{-11}	28
(3)	$F + H_2 \rightarrow HF(3) + H$	1.20×10^{-11}	28
(4)	$H + NF_2 \rightarrow HF(0) + NF(a)$	8.00×10^{-12}	28
(5)	$H + NF_2 \rightarrow HF(1) + NF(a)$	3.00×10^{-12}	28
(6)	$H + NF_2 \rightarrow HF(2) + NF(a)$	7.70×10^{-13}	28
(7)	$H + NF_2 \rightarrow HF(3) + NF(a)$	1.20×10^{-13}	28
(8)	$H + NF_2 \rightarrow HF(0) + NF(b)$	2.60×10^{-13}	28
(9)	$H + NF_2 \rightarrow N_2(B) + NF(X)$	9.10×10^{-13}	28
(10)	$H + NF(a) \rightarrow HF(0) + N(^2D)$	3.10×10^{-13}	6
(11)	$H + NF(b) \rightarrow H + NF(a)$	5.00×10^{-12}	28
(12)	$HF(2) + NF(a) \rightarrow NF(b) + HF(0)$	8.30×10^{-12}	28
(13)	$HF(3) + NF(a) \rightarrow NF(b) + HF(1)$	7.50×10^{-11}	28
(14)	$HF(4) + NF(a) \rightarrow NF(b) + HF(2)$	3.30×10^{-12}	28
(15)	$N(^2D) + NF(a) \rightarrow N_2(B) + F$	1.90×10^{-10}	this work[b]
(16)	$HF(1) + HF(1) \rightarrow HF(0) + HF(2)$	1.70×10^{-11}	28
(17)	$HF(1) + HF(2) \rightarrow HF(0) + HF(3)$	2.00×10^{-11}	28
(18)	$HF(1) + HF(3) \rightarrow HF(0) + HF(4)$	2.20×10^{-11}	28
(19)	$HF(4) + HF(0) \rightarrow HF(3) + HF(0)$	4.30×10^{-11}	28
(20)	$HF(3) + HF(0) \rightarrow HF(2) + HF(0)$	2.00×10^{-11}	28
(21)	$HF(2) + HF(0) \rightarrow HF(1) + HF(0)$	7.20×10^{-12}	28
(22)	$HF(1) + HF(0) \rightarrow HF(0) + HF(0)$	1.20×10^{-12}	28
(23)	$HF(4) + H_2 \rightarrow HF(3) + H_2$	8.50×10^{-13}	28
(24)	$HF(3) + H_2 \rightarrow HF(2) + H_2$	3.90×10^{-13}	28
(25)	$HF(2) + H_2 \rightarrow HF(1) + H_2$	1.30×10^{-13}	28
(26)	$HF(1) + H_2 \rightarrow HF(0) + H_2$	2.00×10^{-14}	28
(27)	$HF(1) + NF_2 \rightarrow HF(0) + NF_2$	1.40×10^{-14}	28
(28)	$HF(2) + NF_2 \rightarrow HF(1) + NF_2$	9.70×10^{-14}	28
(29)	$HF(3) + NF_2 \rightarrow HF(2) + NF_2$	2.50×10^{-13}	28
(30)	$HF(4) + NF_2 \rightarrow HF(3) + NF_2$	5.80×10^{-13}	28
(31)	$NF(b) + \rightarrow NF(X) + h\nu$	$4.50 \times 10^{+01}$	28
(32)	$F + NF_2 + M \rightarrow NF_3 + M$	1.00×10^{-30}	28
(33)	$NF(a) + NF_2 \rightarrow NF(X) + NF_2$	2.70×10^{-16}	28
(34)	$N_2(B) + \rightarrow N_2(A) + h\nu$	$1.50 \times 10^{+05}$	28
(35)	$N_2(A) + WALL \rightarrow N_2(X)$	$2.18 \times 10^{+02}$	calcd[c]
(36)	$N(^2D) + WALL \rightarrow N(^4S)$	$2.34 \times 10^{+02}$	calcd[c]
(37)	$N(^2D) + H_2 \rightarrow N(^4S) + H_2$	2.30×10^{-12}	9
(38)	$N(^2D) + NF_3 \rightarrow N(^4S) + NF_3$	3.00×10^{-13}	this work[d]
(39)	$N(^4S) + NF_2 \rightarrow NF(X) + NF(X)$	3.00×10^{-12}	3
(40)	$N_2(A) + N_2(A) \rightarrow N_2(B) + N_2(X)$	7.70×10^{-11}	14
(41)	$N_2(A) + N_2(A) \rightarrow N_2(C) + N_2(X)$	15.6×10^{-11}	8
(42)	$NF(a) + WALL \rightarrow NF(X)$	100	e

[a] Units cm^3 $molecule^{-1}$ s^{-1} except reactions 31, 34, 36, and 42 which have units of s^{-1}. [b] Reduced from value in text to account for $N_2(B)$ quenching. [c] Diffusional loss. [d] Unpublished measurement. [e] Model parameter.

molecular hydrogen was introduced into the flow tube, atomic hydrogen is produced by the reaction of $F + H_2$.

As pointed out previously, when H_2 is added to the products of the NF_3 discharge, [NF(a)] rises and then reaches a plateau which is independent of further H_2 increases. This titration end point is interpreted to occur when all F has been consumed, i.e., $[H_2]_0 \sim [F]_0$. Examination of the data in this manner indicates that approximately four F atoms must be produced by the discharge for every five NF_3 molecules that are introduced into the cavity.

The estimate for $[NF_2]_0$ is less certain. Since this model best fits the data when $[NF_2]_0/[F]_0 \sim 1/2$, it appears that the microwave discharge produces about a 50% yield of NF_2 from the NF_3. Note that the discharge is always run at a relatively low power, ~10 W. When the discharge power was increased to 30 W, the NF(a) and $N_2(B)$ concentrations were drastically reduced, indicating that at high microwave fluxes NF_2 is dissociated. In addition, $N(^4S)$ (detected at 120 nm by resonance fluorescence) increased as the microwave power increased.

Figure 9 compares predicted and measured profiles of NF(a), $N(^2D)$, and $N_2(B)$ using the rate determined previously[6] for reaction 2 and that determined here for reaction 3. Given that the estimated uncertainties for these two rate coefficients are ~20% and 40%, respectively, the agreement is quite good.

An empirical removal rate (100 s^{-1}) for NF(a) was included to obtain the predicted profiles. The actual source of this removal is not presently understood. Although we list it as a wall reaction, Cheah and Clyne's[5] observations indicate that wall removal of NF(a) is not efficient. Recent results from Quiñones et al.[29]

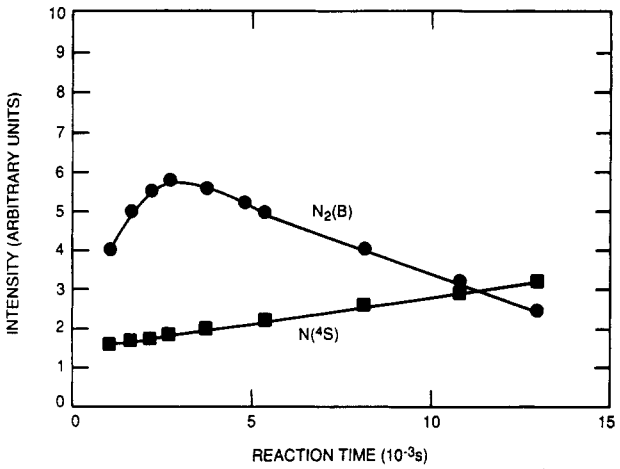

Figure 9. Temporal profiles of $N_2(B)$ and $N(^4S)$ produced in the $H + NF_2$ reaction sequence.

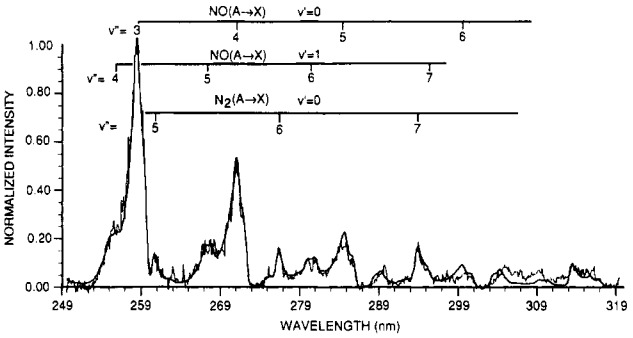

Figure 10. Chemiluminescence spectrum (dark line) and spectral fit (light line) produced from the $H + NF_2$ reaction sequence. Prominent features are assigned.

showed that wall quenching of NF(a) on halocarbon-coated walls is slow, $k_w \sim 0.2$ s^{-1}. This removal of NF(a) is an open question, and the possibility of some bimolecular reaction must be considered. It is significant to note that Cheah and Clyne observed an NF(a) removal rate of 75–150 s^{-1} that they attributed to quenching. The recent work of Quiñones et al.[29] and Benard and co-workers[30] indicates that the NF(a) + NF(a) process is too slow to account for a first-order removal rate on the order of 100 s^{-1}. More work is indicated.

The model supports two important features of the proposed $H + NF_2$ mechanism. First, it is consistent with a two-step production of $N_2(B)$ via reactions 2 and 3 with $k_2 \ll k_3$. Second, it supports the hypothesis that the branching ratio for $N(^2D)$ production in reaction 2 is essentially unity.

C. Additional Observations. We also investigated the production of $N_2(A^3\Sigma_u^+)$ from the $H + NF_2$ sequence by recording both $N_2(A \rightarrow X)$ and $N_2(B \rightarrow A)$ chemiluminescence. Figure 10 shows the spectrum between 250 and 320 nm and the spectral fit for $N_2(A \rightarrow X)$ and $NO(A \rightarrow X)$. The latter emission is excited by energy transfer from $N_2(A)$ to NO,[31] NO being an impurity that is created in the NF_3 discharge. The $N_2(A)$ number densities we measured ranged from 2×10^9 to 8×10^9 molecules cm^{-3} for a variety of conditions. The highest concentrations were obtained at relatively high pressures (~1 Torr) where wall losses would be minimized. Typically, $[N_2(A)]$ exceeded $[N_2(B)]$ by about 2 orders of magnitude. This is in qualitative agreement with our modeling predictions which have $N_2(B \rightarrow A)$ emission as the only source of $N_2(A)$. It appears, therefore, that the dominant production process for $N_2(A)$ is $N_2(B \rightarrow A)$ radiative cascade.

(29) Quiñones, E.; Habdas, J.; Setser, D. W. *J. Phys. Chem.* **1987**, *91*, 5155.
(30) Benard, D. J.; Winkler, B. K.; Seder, T. A.; Cohn, R. H. *J. Phys. Chem.* **1989**, *93*, 4790.
(31) Piper, L. G.; Cowles, L. M.; Rawlins, W. T. *J. Chem. Phys.* **1986**, *85*, 3369.

Hoping to produce higher $[N_2(A)]$ by accelerating the rate of reaction 2, we added H atoms directly to the reactor by discharging the H_2 flow. The $[N_2(A)]$ was degraded by a factor of 2. Apparently, H atom quenching of $N_2(A)$ or a precursor is a serious problem. Hovis and Whitefield[32] reported a rate coefficient of 5×10^{-11} cm^3 molecule^{-1} s^{-1} for quenching $N_2(A,v'=0)$ by H. The quenching reaction to form NH + N from $N_2(A,v=0)$ is slightly endothermic ($\approx 3kT$).[33] Hack et al.[34] have shown that NH is not a product of this quenching. One quantum of vibrational energy in $N_2(A)$, however, would make this process exothermic. The vibrational energy might open a reactive channel to make the rate even faster. To our knowledge no one has looked for this effect.

D. Related Studies. Cheah and Clyne[5] and Hovis et al.[35] have also investigated the kinetics of $N_2(B)$ formation in the H + NF_2 flame. Cheah and Clyne demonstrated clearly that the $N_2(B)$ photon emission rates varied linearly with the product of the number densities of $NF(a^1\Delta)$ and $N(^2D)$. They suggested that the $N_2(B)$ intensities they observed indicated a rate coefficient for k_3 on the order of one-tenth gas kinetic, i.e., $\approx 3 \times 10^{-11}$ cm^3 molecule^{-1} s^{-1}. Their photometric calibrations were sufficiently imprecise, however, that our measured value of k_3, which is an order of magnitude larger than Cheah and Clyne's estimate, is fully consistent with their observations.

Cheah and Clyne reported an $N_2(B)$ vibrational distribution that declined more or less uniformly with increasing vibrational energy. It could be characterized moderately well with a Boltzmann temperature of 8200 K. Their measurements were made in an argon bath gas. Our observations, which are summarized in Figure 5, show that an argon bath will relax the initial $N_2(B)$ vibrational distribution substantially. Their result, therefore, is not in conflict with our distributions displayed in Figure 4 and summarized in Table I.

Hovis et al. made their observations in helium, and the relative vibrational distribution they report agrees excellently with our own with the exception of vibrational levels 11 and 12. Their fractional populations for these vibrational levels respectively are 40% and 75% larger than those we have measured.

They also reported a relative population for $v' = 0$. Normalizing their results for $v' = 1-12$ with ours indicates that inclusion of their value for $v' = 0$ would result in a 16% increase to our total excitation rate coefficient. That is, including their value for $v' = 0$ gives $k_3 = (2.9 \pm 1.3) \times 10^{-10}$ cm^3 molecule^{-1} s^{-1}.

Hovis et al. estimated that the rate coefficient for reaction 3 is on the order of 1×10^{-10} cm^3 molecule^{-1} s^{-1}. This agrees adequately with our own measurement which is more direct.

The bimodal vibrational distribution for $N_2(B)$ that is displayed in Figure 4 might indicate that $N_2(B)$ is formed by two different reactions. Vibrational levels above $v' = 6$ are energetically accessible only via reaction 3. The lower vibrational levels, however, could conceivably be produced in reaction 9, i.e., the reaction between $N(^2D)$ and $NF(X^3\Sigma_u^-)$.

Cheah and Clyne[4] estimated the branching fraction in reaction 1 to be ≥ 0.9 for producing $NF(a^1\Delta)$. Malins and Setser[13] concurred with this estimate and indicated furthermore that the branching fraction for producing NF(X) in reaction 1 was likely less than 0.07.

Hovis et al.[35] recently questioned whether 90% of reaction 1 really does make NF(a). Their data indicate a somewhat lower branching fraction. However, the question of the H + NF_2 branching ratio seems to have been answered by a recent series of elegant experiments by Heidner et al.[36] They developed a laser-induced fluorescence technique for monitoring NF(X) and were able to place a lower limit for the product branching ratio of H + NF_2; $[NF(a)]/[NF]_{tot} > 0.99$. We feel confident, therefore, NF(X) should be a minor species in our system, and reaction 9 is unlikely to contribute significantly to our observations.

An alternative explanation for the strange $N_2(B)$ vibrational distribution that is observed could be that the distribution is distorted by collisional coupling into the nearly resonant levels of longer lived electronic states of nitrogen. These states would include $W^3\Delta_u$, $B'^3\Sigma_u^-$, and $A^3\Sigma_u^+$. Such coupling has been demonstrated previously in laser excitation experiments by Rotem and Rosenwaks[37] and Sadeghi and Setser.[38] Our results in helium should reduce this coupling but may not eliminate it.

A final possibility for the bimodal $N_2(B)$ vibrational distribution is that $N_2(B)$ is formed directly in reaction 3, but with a vibrational distribution that peaks at $v' = 6$ and falls off to both lower and higher vibrational levels. A second channel could populate $N_2(B'^3\Sigma_u^-)$. Radiative and collisional cascade from this state, then, would populate the lower levels of $N_2(B)$. We did not observe significant radiation from the infrared afterglow system, $N_2(B'^3\Sigma_u^- - B^3\Pi_g)$, but most of the important transitions of this system would have been outside the sensitivity limits of our detection system. A similar suggestion has been proposed to explain the excitation of $N_2(B)$ from the reaction between $Ar^*(^3P_{0,2})$ and N_2O.[39] These latter studies were performed at pressures in the milliTorr region where collisional effects should be minimal.

V. Conclusions

We have shown that the rate coefficient for producing $N_2(B^3\Pi_g)$ in the reaction between $N(^2D)$ and $NF(a^1\Delta)$ is essentially gas kinetic. This reaction produces $N_2(B)$ up to the nitrogen dissociation limit. The $N_2(A)$ observed to be produced in this system appears to result primarily from radiative cascade from $N_2(B)$.

All N_2^* appears to be produced by reaction 3. Since reaction 3 is exothermic enough to produce excitation up to the dissociation limit, and since production of N_2^* is indeed observed all the way to this limit, there is likely an inherent inefficiency in the system with respect to partitioning into specific N_2^* states.

Acknowledgment. We appreciate financial support from the Air Force Weapons Laboratory under Contract No. F29601-84-C-0076. We enjoyed illuminating discussions with and critical comments from Dave Green, Terry Rawlins, George Caledonia, Bill Marinelli, and Mark Fraser and found Margrethe DeFaccio's analytical support invaluable.

Registry No. N, 17778-88-0; NF, 13967-06-1.

(32) Hovis, F. E.; Whitefield, P. D. *Chem. Phys. Lett.* **1987**, *138*, 162.
(33) Piper, L. G. *J. Chem. Phys.* **1979**, *70*, 3417.
(34) Hack, W.; Kurzke, H.; Ottinger, Ch.; Wagner, H. Gg. *Chem. Phys.* **1988**, *126*, 111.
(35) Hovis, F. E.; Whitefield, P. D.; Lilenfeld, H. V.; Bradburn, G. R. *J. Phys. Chem.* **1988**, *92*, 5133.
(36) Heidner, R. F.; Helvajian, H.; Holloway, J. S.; Koffend, J. B. Presented at the AIAA Thermophysics, Plasmadynamics, and Lasers Conference, San Antonio, TX, 1988; paper AIAA-88-2758.
(37) Rotem, A.; Rosenwaks, S. *Opt. Eng.* **1983**, *22*, 564.
(38) Sadeghi, N.; Setser, D. W. *J. Chem. Phys.* **1983**, *79*, 2710.
(39) Wu, K. T.; Cummings, W. P.; Piper, L. G. *J. Phys. Chem.*, submitted for publication.